NORRESTAM, R., HOVMOLLER, S., PALM, T.-B., GOTHE, R. & WACHTMEISTER, C. A. (1977). *Acta Cryst.* B33, 370–376.
PENTO, J. T., MAGARIAN, R. A. & KING, M. M. (1982). *Cancer Lett.* **15**, 261–269.
PENTO, J. T., MAGARIAN, R. A., WRIGHT, R. J., KING, M. M. & BENJAMIN, E. J. (1981). *J. Pharm. Sci.* **70**, 399–403.
POPPLETON, B. J. (1986). *Acta Cryst.* C42, 879–881.
PRECIGOUX, G., COURSEILLE, C., GEOFFRE, S. & HOSPITAL, M. (1979). *Acta Cryst.* B35, 3070–3072.
ROGERS, M. T. & ROBERTS, J. D. (1946). *J. Am. Chem. Soc.* **68**, 843–846.
ROMMING, C. & SYDNES, L. K. (1987). *Acta. Chem. Scand. Ser. B*, **41**, 717–723.
SCHRUMPF, G. & JONES, P. G. (1987*a*). *Acta Cryst.* C43, 1182–1185.
SCHRUMPF, G. & JONES, P. G. (1987*b*). *Acta Cryst.* C43, 1185–1187.
SHELDRICK, G. M. (1976). *SHELX*76. Program for crystal structure determination. Univ. of Cambridge, England.
SUTHERLAND, R. L. & JORDAN, V. C. (1981). Editors. *Non-Steroidal Antiestrogens*. Sydney: Academic.
TINANT, B., DECLERCQ, J.-P. & VAN MEERSSCHE, M. (1985). *Acta Cryst.* C41, 597–599.
TINANT, B., TOUILLAUX, R., DECLERCQ, J.-P., VAN MEERSSCHE, M., LEROY, G. & WEILER, J. (1983). *Bull Soc. Chim. Belg.* **92**, 101–110.
TINANT, B., WU, S., DECLERCQ, J.-P., VAN MEERSSCHE, M., MASAMBA, W., DE MESMAEKER, A. & VIEHE, H. G. (1988). *J. Chem. Soc. Perkin Trans.* 2, pp. 1045–1052.
WEEKS, C. M., GRIFFIN, J. F. & DUAX, W. L. (1977). Am. Crystallogr. Assoc. Summer Meet., Abstract PB6.
ZUKERMAN-SCHPECTOR, J., CASTELLANO, E. E., OLIVA, G., BROCKSOM, T. J. & CANEVAROLO, E. T. (1984). *Can. J. Chem.* **62**, 570–573.

Acta Cryst. (1991). B47, 521–527

X-ray Analysis of Cubic Crystals of the Complex Formed Between Ribonuclease T_1 and Guanosine-3′,5′-bisphosphate

BY ANDREA LENZ, UDO HEINEMANN, MARIA MASLOWSKA AND WOLFRAM SAENGER

Institut für Kristallographie, Freie Universität Berlin, Takustr. 6, *D*-1000 *Berlin* 33, *Germany*

(*Received* 2 *August* 1990; *accepted* 30 *January* 1991)

Abstract

The complex formed between ribonuclease T_1 (RNase T_1) and guanosine-3′,5′-bisphosphate (3′,5′-pGp) crystallizes in the cubic space group $I23$ with $a = 86{\cdot}47$ (4) Å. X-ray data were collected on a four-circle diffractometer to 3·2 Å resolution and the structure was determined by molecular-replacement methods [*ULTIMA*; Rabinovich & Shakked (1984). *Acta Cryst.* A40, 195–200] based on the RNase T_1 coordinates taken from the complex with guanosine-2′-phosphate. Refinement converged at 16·6% for 1540 data with $|F_o| > 1\sigma(|F_o|)$ with acceptable stereochemistry. The RNase T_1 conformation is comparable to that in other complexes which crystallize preferentially in space group $P2_12_12_1$ except for side chains that interact intermolecularly. The guanine of 3′,5′-pGp is bound to the recognition site in the same way as in other guanine-containing complexes except for its interaction with Glu46. The side-chain carboxylate of this amino acid does not form hydrogen bonds to N1H and N2H of guanine but is rotated so as to permit insertion of two water molecules which replace its acceptor functions. In contrast to other guanosine derivatives which are bound to RNase T_1 in the *syn* form, 3′,5′-pGp is *anti*. This conformation positions the two phosphate groups 'outside' the protein, with hydrogen-bonding contacts only to water molecules; the active site is filled by water. The RNase T_1–3′,5′-pGp complex probably has biological significance as it may represent the enzyme–product complex before dissociation.

Introduction

Although ribonuclease T_1 (RNase T_1) from the fungus *Aspergillus oryzae* with a chain length of only 104 amino acids is one of the smallest known enzymes, it is highly specific (Takahashi & Moore, 1982; Heinemann & Hahn, 1989). It cleaves RNA at the 3′-phosphate position of guanosine, yielding through transesterification oligonucleotides with terminal guanosine-2′,3′-cyclic phosphates which are ultimately hydrolyzed to oligonucleotides with a terminal 3′-guanylic acid. The reaction is catalyzed by Glu58, Arg77, His92; His40 appears to serve as an activator for Glu58 (Heinemann & Saenger, 1982). The specific recognition between RNase T_1 and guanine is through a combination of hydrogen bonds formed between Asn43N^{δ}H···N7, Asn44NH···O6, Tyr45NH···O6, Glu46$O^{\epsilon 1}$···HN1, Glu46$O^{\epsilon 2}$···H_1N2, Asn98O···H_2N2, and stacking interactions whereby guanine is sandwiched between the side chains of Tyr42 and Tyr45 (Arni, Heinemann, Tokuoka & Saenger, 1988).

This detailed knowledge was obtained by spectroscopic and, notably, by crystallographic studies in

0108-7681/91/040521-07$03.00

which the complexes formed by RNase T_1 and the inhibitors guanosine-2′-phosphate (2′-GMP) and guanylyl-2′,5′-guanosine [Gp(2′,5′)G] were investigated (Arni, Heinemann, Tokuoka & Saenger, 1988; Koepke, Maslowska, Heinemann & Saenger, 1989). The guanylic acid bound to the active site is not in the generally preferred *anti* conformation with the guanine rotated away from the ribose moiety (Saenger, 1984) but adopts the *syn* form which allows the ribose O5′H group to interact intramolecularly with the guanine N3 atom through a hydrogen bond. This conformation was also determined in solution experiments using CD and NMR spectroscopy (Oshima & Imahori, 1972; Inagaki, Shimada & Miyazawa, 1985; Hoffmann, Schmidt, Simon & Rüterjans, 1988).

Guanosine-3′,5′-bisphosphate (3′,5′-pGp) is a model for the product of RNA cleavage by RNase T_1 as it represents one short fragment of RNA with terminal 3′- and 5′-phosphate groups. It was surprising that spectroscopic studies had indicated nucleotides with a 5′-phosphate group to bind in *anti* form to RNase T_1 (Inagaki, Shimada & Miyazawa, 1985; Shimada & Inagaki, 1990). In order to verify this finding and to establish the nature of the enzyme–nucleotide interactions, the X-ray study described below was carried out.

Materials and methods

RNase T_1 was isolated from an extract of *A. oryzae* (Fülling & Rüterjans, 1978). For the crystallization, the lyophilized enzyme was dissolved at 1% concentration in 10 m*M* sodium acetate buffer at pH 4·2, containing 2 m*M* calcium acetate and 0·25% 3′,5′-pGp. This solution was mixed with 2-methyl-2,4-pentane-diol (MPD) to yield a concentration of 40% MPD, and dialyzed by a micro technique (Dattagupta *et al.*, 1975) against the same buffer containing 50–58% MPD (Heinemann, 1982). Cube-shaped crystals appeared after one week and their edges grew to around 0·4 mm within four weeks.

The crystals are not birefringent under polarized light, suggesting a cubic space group. Unit-cell constants $a = b = c = 86{\cdot}47\ (4)$ Å were determined from diffractometer angular settings of 20 reflections, and precession photographs indicated systematic extinction conditions $h + k + l = 2n + 1$. For proteins these are satisfied by two cubic space groups, $I23$ (No. 197) and $I2_13$ (No. 199). Both contain 24 asymmetric units and are consistent with the cell volume and molecular weight of RNase T_1, giving an acceptable value of 2·43 Å^3 per dalton. In other crystal structures of native or complexed RNase T_1, the space group is predominantly $P2_12_12_1$ (No. 19) (Heinemann & Hahn, 1989) which is a subgroup of No. 199.

X-ray data were collected from one single crystal (0·35 × 0·35 × 0·35 mm) using a Stoe four-circle diffractometer equipped with a sealed copper tube, λ = 1·54178 Å, operated at 40 kV and 35 mA. In a quadrant of reciprocal space, reflections were measured in the ω-scan mode with stationary background counts on both sides of each scan. Three reference reflections were measured at hourly intervals. The reflection data were only collected to 3·2 Å resolution because their intensities fell off rapidly beyond this limit. This fall-off originates mostly from limited crystalline order since it is sharp, and low-angle reflections are fairly strong. The data were corrected for Lorentz and polarization factors and for absorption using the semi-empirical method of North, Phillips & Mathews (1968). With 1645 observed reflections [$|F_o| \geq 1\sigma(|F_o|)$] the final data set contains 87% of the data expected at 3·2 Å resolution. The internal agreement is $R_{sym} = \sum||F| - \langle|F|\rangle|/\sum|F| = 4{\cdot}3\%$, based on 4274 multiple measurements in 1408 unique reflections.

Structure determination

If the three-dimensional structure of a protein is known, a crystal structure of the protein itself or complexed with a substrate can be determined using molecular-replacement methods (Rossmann, 1972). In these methods, Patterson search is employed to establish the rotation and translation of the protein in the actual space group. Since most of the search programs are not suitable for high-symmetry space groups (Fitzgerald, 1988) we used the real-space multi-dimensional search program *ULTIMA* (Rabinovich & Shakked, 1984). Based on the protein atomic coordinates of the RNase T_1–2′-GMP complex, the search was carried out in the two possible space groups $I23$ and $I2_13$. By trial-and-error approaches, the most sensitive resolution for the search routines was found to be in the 20–10 Å range. A translational search grid of 1/40 of the unit-cell axial length and a rotational grid of 30° were used. The parameter space searched was as given by Hirschfeld (1968).

The global maximum yielded rotation and translation parameters which positioned the RNase T_1 molecule in the asymmetric unit. An intermolecular-distance calculation indicated that there were no close contacts or even atom overlaps. Using amino-acid group scattering factors in initial stages with the subroutine *LOOP*, the position and orientation of the 40 best trial structures were refined with stepwise increase in resolution: 20–10, 15–8, 10–6 Å. The best seven sets ($R \leq 49\%$) were finally refined as rigid structures with reflections in the 10–3·5 Å range. Atomic scattering factors were used instead of group scatterers, because at resolutions < 6 Å the

difference between these scattering factors becomes significant (Rabinovich & Shakked, 1984). Convergence to the lowest R factor (34%) indicated that the correct solution was to be found in space group $I23$ (No. 197). At this stage, the next best solution yielded $R = 52\%$. In the same resolution range, no solution in space group $I2_13$ gave an R value below 50%. Therefore, the choice of space group $I23$ was unequivocal. To the best of our knowledge, this is the first determination of an unknown protein structure using the *ULTIMA* approach, although the use of the program to determine nucleic acid structures is well documented (Kennard & Hunter, 1989).

Refinement continued with *PROFFT* (Hendrickson & Konnert, 1980; Hendrickson, 1985; Finzel, 1987). Owing to the medium resolution of the available X-ray data, atomic temperature factors were not refined individually. Instead, overall starting B values of 10, 12 and 25 Å^2 for main-chain, side-chain and solvent atoms, respectively, were found by trial and error. During refinement the values were incremented with the overall temperature factor shifts indicated to yield final overall B values of 8·02, 10·02 and 23·02 Å^2 for the three classes of atoms. In this scheme, the bound nucleotide was treated like a protein side chain.

Fourier and difference Fourier maps were calculated periodically after several rounds of refinement in order to control the geometry of RNase T_1 and to locate 3′,5′-pGp and water molecules. The program *FRODO* (Jones, 1978), installed on an Evans & Sutherland PS390 graphics display, was used. Special attention was paid to the positioning of active-site side chains which were rebuilt to fit omit maps whenever the fit to the electron density seemed poor. The position and conformation of the bound pGp was clearly revealed in difference density maps.

Difference density peaks above 0·25 e Å^{-3} were assigned as water oxygens if their positions were within 3·4 Å from protein or nucleotide O or N or other water O atoms. One water oxygen (Wat200) is located on a C_2 axis and was set to an occupation of $\frac{1}{2}$. All other water sites were kept at occupation factors of 1·0. Water positions were removed from the atom list when displaying poor electron density and failing to reappear in subsequent omit maps. Several water positions thus identified are conserved in RNase T_1 crystal structures (Malin, Zielenkiewicz & Saenger, 1991).

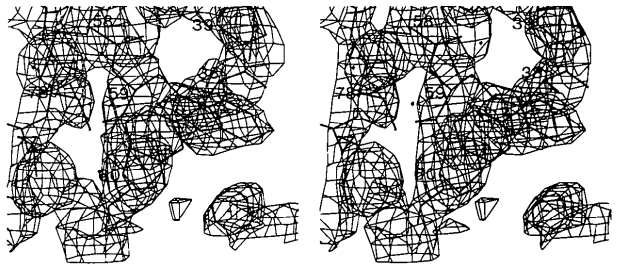

Fig. 1. Stereoview of a representative portion of the $2|F_o| - |F_c|$ electron density map contoured at 0·48 e Å^{-3}.

Table 1. *Crystallographic and stereochemical refinement parameters*

The R factor is defined as $\Sigma||F_o| - |F_c||/\Sigma|F_o|$ and the correlation coefficient is $\Sigma[(|F_o| - \langle|F_o|\rangle)(|F_c| - \langle|F_c|\rangle)]/[\Sigma(|F_o| - \langle|F_o|\rangle)^2\Sigma(|F_c| - \langle|F_c|\rangle)^2]^{1/2}$. For the stereochemical parameters the left-hand number gives the r.m.s. deviation from ideality and the right-hand number is the target variance.

Resolution range (Å)	10–3·2
Number of reflections (1σ on $\|F_o\|$)	1540
(3σ on $\|F_o\|$)	1470
R factor (1σ on $\|F_o\|$) (%)	16·6
(3σ on $\|F_o\|$) (%)	16·2
F_o/F_c correlation coefficient	0·882
Bond distances (Å)	0·010/0·020
Bond-angle distances (Å)	0·054/0·050
Planar 1–4 distances (Å)	0·045/0·050
Planar groups (Å)	0·005/0·015
Chiral volumes (Å^3)	0·144/0·150
Single torsion contacts (Å)	0·129/0·150
Multiple torsion contacts (Å)	0·134/0·150

The final model includes 781 atoms from the enzyme, 28 from the nucleotide, and 83 water oxygens. The R factor converged at 16·6% for the 1540 reflections with $|F_o| > 1\sigma(|F_o|)$ between 10 and 3·2 Å resolution.* Omitting the water oxygens from the structure-factor calculation raises the R value to 24·3%. The protein electron density is generally satisfactory, but fine details are not revealed due to the limited resolution. A representative fragment of electron density is displayed in Fig. 1. Table 1 summarizes crystallographic and stereochemical refinement paramaters of the RNase T_1–3′,5′-pGp complex. For the hydrogen-bonding analysis, the positions of H atoms were calculated with the program *MOLEDT* (Biosym Technologies, 1988) (assumed pH of 4·2) for the protein and with *CHEMX* (Chemical Design Ltd, 1990) for the bound nucleotide.

Results and discussion

Conformation and crystal packing of RNase T_1

Compared with the other three published crystal structures, *viz* RNase T_1–2′-GMP (Arni, Heinemann, Tokuoka & Saenger, 1988), RNase T_1–Gp(2′,5′)G

* Atomic coordinates and structure factors have been deposited with the Protein Data Bank, Brookhaven National Laboratory (Reference: 5RNT, R5RNTSF), and are available in machine-readable form from the Protein Data Bank at Brookhaven. The data have also been deposited with the British Library Document Supply Centre as Supplementary Publication No. SUP 37043 (as microfiche). Free copies may be obtained through The Technical Editor, International Union of Crystallography, 5 Abbey Square, Chester CH1 2HU, England. At the request of the authors, the list of structure factors will remain privileged until 31 December 1993.

(Koepke, Maslowska, Heinemann & Saenger, 1989) and RNase T_1–vanadate (Kostrewa, Choe, Heinemann & Saenger, 1989) which all crystallized in space group $P2_12_12_1$, the conformation of RNase T_1 in the cubic space group (Fig. 2) is nearly identical. This is shown in Fig. 3 where the r.m.s. deviations between the atomic coordinates of the two RNase T_1 structures in the 2′-GMP and the present complex are given. In the main-chain geometry, most of the deviations are in loop regions (30–33), (68–74) and (95–100), which we associate with packing effects. In the side chains, there are several major deviations, *viz* Lys25, Ser72, Asn98. These are in direct intermolecular contact in this cubic structure (Lys25; Table 2) or in the other orthorhombic crystal structures (Ser72, Asn98) so that the geometrical discrepancies are readily explained.

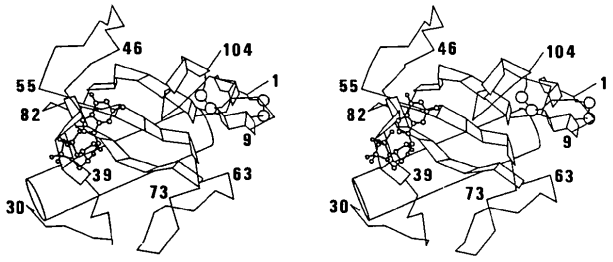

Fig. 2. Stereoview displaying schematically the structure of the RNase T_1–3′,5′-pGp complex. This figure was produced using a program written by Lesk & Hardman (1982).

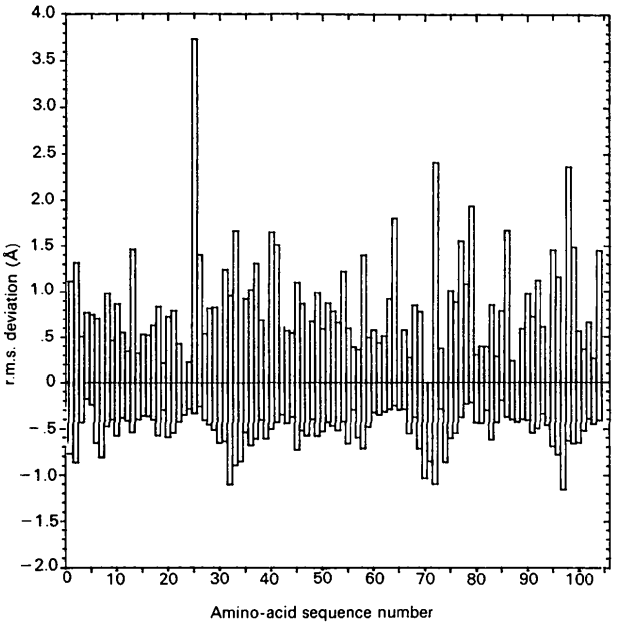

Fig. 3. Root-mean-square deviation (Å) for main-chain (bottom) and side-chain (top) atoms, as a function of amino-acid sequence. Compared are RNase T_1–3′,5′-pGp and RNase T_1–2′-GMP.

Table 2. *Possible intermolecular hydrogen bonds* ≤3·5 Å *for RNase* T_1–3′,5′-*pGp*

T_x, T_y and T_z refer to translation in x, y and z respectively.

Residue···Residue	Distance (Å)	*D*—H···*A* (°)	Symm*	T_x	T_y	T_z
Asn44O···N Gly34	3·1	150	23	0	0	0
Tyr45O···N Gly97	3·4	138	7	1	0	0
Asp49$O^{\delta1}$···N^{ζ}Lys25	3·0		6	1	1	0
Asp49$O^{\delta2}$···O^{γ}Ser35	3·4		23	0	0	0
Ser54O^{γ}···O Ser69	3·0		23	0	0	0
Ser54O^{γ}···O^{γ}Ser69	3·4		23	0	0	0
Ser54O^{γ}···O Gly70	2·9		23	0	0	0
Asn99$N^{\delta2}$···O Ser96	2·8	144	7	1	0	0

* Symmetry operations: (6) $-z, -x, y$; (7) $-x, y, z$; (23) $\frac{1}{2}+y, \frac{1}{2}-z, \frac{1}{2}-x$.

The mutual orientation and packing of the RNase T_1 molecules is very different in space groups $I23$ and $P2_12_12_1$. In the former, molecules are related by two- and threefold rotation axes, in the latter by 2_1 screw axes. Also, the packing density is different, 2·43 $Å^3$ per dalton in $I23$ and 2·14 $Å^3$ per dalton in $P2_12_12_1$ (assuming equal crystal density), so that packing in $I23$ is not as tight as in $P2_12_12_1$ and consequently the degree of hydration is higher. This and the larger number (24) of molecules in the unit cell might be the reason why the resolution of the $I23$ crystals is inferior to that of the crystals with the lower-symmetry space group.

Anti conformation of the nucleotide

The most striking difference between the three RNase T_1–nucleotide structures is in the conformation of the nucleotide (Table 3). It is *anti* in the present complex but *syn* in the other two. There is no doubt that the conformer is *anti* as the two phosphate groups and the ribose and base moieties are located in well-defined density, see Fig. 4. At the resolution of the analysis, nucleotide torsion angles can only be estimated. The sugar pucker is determined mainly from the positions of the phosphate groups which have difference electron density at the 0·5 e $Å^{-3}$ level. Difference density maps contoured at 0·35 e $Å^{-3}$ clearly define the base and sugar orientations. The positions of the phosphate oxygens are not revealed and were adjusted so as to avoid bad van der Waals contacts. The sugar adopts a pucker near or at the C3′-*endo* domain, the torsion angle β, $\sim -80°$, puts the 5′-phosphate group in a semiextended position, and γ and ε adopt conventional $+$*gauche* and *anti* forms, respectively.

In the electron density maps, five water molecules could be located within hydrogen-bonding distance of the phosphate O atoms. In the rotational setting chosen, the 3′-phosphate group is associated with three water molecules, of which Wat174 and Wat125 are further hydrogen bonded to Tyr45O, and to

Table 3. *Approximate torsion angles* (°) *of* 3′,5′-*pGp and pseudorotation parameters* (°) (*Altona & Sundaralingam*, 1972)

P—O5′—C5′—C4′		(β)	−80	
O5′—C5′—C4′—C3′		(γ)	50	
C5′—C4′—C3′—O3′		(δ)	80	
C5′—C4′—C3′—C2′			−160	
C4′—C3′—C2′—O2′			−85	
C4′—C3′—O3′—P		(ε)	180	
C4—N9—C1′—O4′		(χ)	−160	(*anti*)
τ_0	−5	τ_3	−50	
τ_1	−25	τ_4	35	
τ_2	−45	P	25	(3′-*endo*)

Glu31O$^{\varepsilon 1,2}$ (of a symmetry-related RNase T_1 molecule), respectively. Similarly, two of the O atoms of the 5′-phosphate group, O2 and O3, chelate Wat139 which is also in contact with the peptide NH of Lys41 (Fig. 5). Since there is 'empty space' around both phosphate groups, we expect more water molecules to be associated, which, however, are not seen in the electron density, at the present resolution.

An interesting structural feature of the 3′,5′-pGp molecule is a potential bifurcated chelate hydrogen-bonding contact between the O atoms of the 3′- and 5′-phosphate groups, O(5P)3′···O(1P), O(3P)5′ at 2·6 and 2·9 Å (Figs. 5, 6 and Table 4). This interaction can also occur with the products of RNase T_1 hydrolysis, *i.e.* oligonucleotides with terminal guanosine-3′-phosphate; it requires that one or two of the oxygens be protonated, as expected for phosphate monoesters at pH 7·0.

Binding of guanine at the recognition site; the 'empty' active site

As shown in Table 4 and in Fig. 5, guanine is bound similarly in the RNase T_1 complexes with 2′-GMP and 3′,5′-pGp, but not identically. It is sandwiched between the side chains of Tyr42 and Tyr45, and the interactions between guanine N7, O6, NH_2 and the protein main-chain groups Asn43NH, Asn44NH, Tyr45NH, Asn98C=O are comparable. The main difference occurs with the Glu46 side chain whose carboxylate O atoms are not in direct hydrogen-bonding contact with N1H and N2H of guanine. Instead, water molecule Wat183 chelates guanine O6, N1H, and Wat172 chelates N1H, N2H; these two water molecules are themselves at a hydrogen-bonding distance of 2·7 Å (Fig. 5 and Table 4). Rotation of the Glu46 side chain away from guanine is probably facilitated by an intramolecular hydrogen bond Glu46O$^{\varepsilon 2}$···HN100Phe, 2·7 Å.

The *anti* conformation of 3′,5′-pGp does not permit the 3′-phosphate to enter the active-site cavity, which is filled by several water molecules (Fig. 6). As in other complexes of RNase T_1, Arg77 and Glu58 are not within hydrogen-bonding distance of each other. In contrast to the other three structures of RNase T_1, where His92N$^{\varepsilon}$H is hydrogen bonded to Asn98 and/or to Asn99 main-chain C=O, the imidazole group in the RNase T_1–3′,5′-pGp complex is only in contact with water molecules. More notable is the possible hydrogen-bonding interaction Glu58O···HN$^{\varepsilon}$His40, 2·8 Å (Table 5) which was not observed in the RNase T_1–2′-GMP complex where

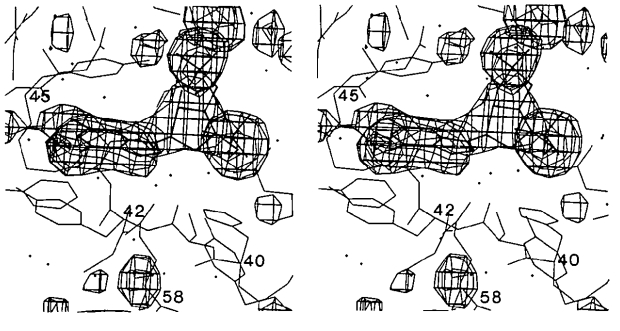

Fig. 4. Stereoview illustrating the electron density for the 3′,5′-pGp molecule. The difference density map shown was computed after several rounds of refinement omitting the 3′,5′-pGp molecule, *i.e.* without phase bias from the nucleotide. The contour level is 0·22 e Å^{-3}, twice the r.m.s. density of the difference map.

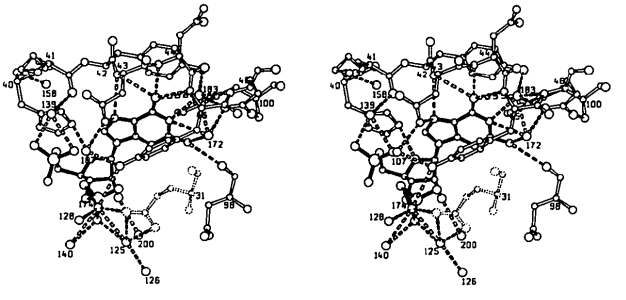

Fig. 5. Stereoview of the guanosine binding site. Glu31 from another asymmetric unit is indicated by dotted lines. Possible hydrogen bonds are given by broken lines.

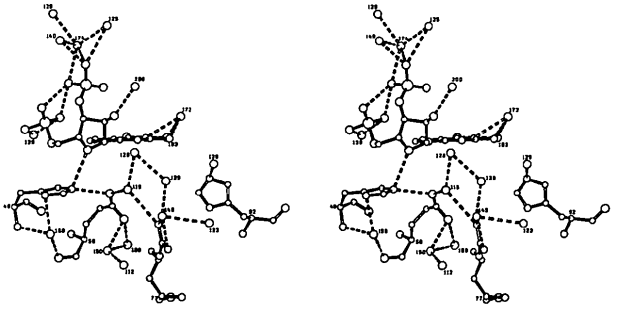

Fig. 6. Stereoview of the catalytic site, with possible hydrogen bonds indicated by dotted lines. Rotation of the ribose moiety about the glycosidic N9—C1′ link into the *syn* conformation would locate the 3′-phosphate group between His92 and Glu58, as required for catalytic action.

Table 4. *Comparison of hydrogen bonding to 3′,5′-pGp and 2′-GMP*

Group	RNase T_1–3′,5′-pGp	Distance (Å)	*D*—H···*A* (°)	RNase T_1–2′-GMP	Distance (Å)	*D*—H···*A* (°)
Guanine	N7···N Asn43	3·4	159	N7···N Asn43	3·3	169
	N7···$N^{\delta 2}$Asn43	3·2	99			
	O6···N Asn43	3·1	103			
	O6···N Asn44	2·7	120	O6···N Asn44	2·8	106
	O6···N Tyr45	3·2	164	O6···N Tyr45	2·8	155
				N1···$O^{\epsilon 1}$Glu46	2·7	161
				N2···$O^{\epsilon 2}$Glu46	3·0	168
	N2···O Asn98	3·3	127	N2···O Asn98	2·9	145
	N1···Wat172[a]	2·9				
	N2···Wat172	2·7				
	N1···Wat183	2·8				
	O6···Wat183	2·9				
Ribose	O4′···$N^{\epsilon 2}$His40	3·0	98			
	O2′···Wat200	2·8		O5′···Wat158	2·8	
	O2′···O1P(3′)	3·1				
5′	O2P[b]···Wat139	2·6		O1P···O^{η}Tyr38	2·7	
	O3P···Wat139	2·9		O1P···$N^{\epsilon 2}$His40	2·8	
	O1P···O5P(3′)	2·9		O1P···$O^{\epsilon 2}$Glu58	3·4	
	O3P···O5P(3′)	2·6				
3′	O2P···Wat125	3·2		O3P···$O^{\epsilon 1}$Glu58	2·7	
	O2P···Wat140	2·7		O3P···$O^{\epsilon 2}$Glu58	2·4	
	O2P···Wat174	2·6		O2P···$O^{\epsilon 2}$Glu58	2·6	
	O5P···Wat174	2·8		O2P···Wat179	3·0	
	O5P···O1P(5′)	2·6		O2P···Wat186	2·7	
	O5P···O3P(5′)	2·9				

Notes: (*a*) Distances: Wat125···Wat174 = 3·0, Wat140···Wat174 = 3·4, Wat172···Wat183 = 2·7 Å. (*b*) Phosphate oxygens.

His40 is associated with the inhibitor 2′-phosphate group. The Glu58···His40 contact was, however, invoked in the mechanistic considerations where His40 was proposed to activate Glu58 so that it becomes a good proton acceptor (Heinemann & Saenger, 1982); this interaction is also observed in the crystal structure of uncomplexed RNase T_1 (Martinez-Oyanedel, Choe, Heinemann & Saenger, 1991).

Concluding remarks

The molecular structure of the RNase T_1–3′,5′-pGp complex has been determined at a resolution of 3·2 Å. Although the limited resolution of this analysis precludes a description of the molecular interactions in fine detail, it is clear that the guanosine glycosyl bond is *anti*, in contrast to the other complexes where the guanosine bound to the active site adopts the *syn* form. The latter is necessary to bring the scissile phosphodiester bond in contact with the catalytic residues His40, Glu58, Arg77, His92. If a substrate binds to RNase T_1 in the *anti* form, no reaction can occur. This means that we have crystallized and investigated a non-productive enzyme–substrate (or rather enzyme–product) complex.

This complex is not an artifact of the crystallization, as indicated by spectroscopic data which suggested that 3′,5′-pGp binds to RNase T_1 in the *anti* form in solution (Inagaki, Shimada & Miyazawa, 1985). The same compound was cocrystallized with an enzyme of the same ribonuclease family, RNase Pb_1. It adopts the *syn* form (Pavlovsky & Karpeisky, 1989) with the 3′-phosphate bound to the amino-acid side chains His40 and His92, and the 5′-phosphate extends freely into solution. We conclude from these data that we observe a complex with biological significance.

What is this significance? If we consider another crystalline complex, RNase T_1–guanosine-3′-phosphate (Sugio, Oka, Ohishi, Tomita & Saenger, 1985) where the ribosephosphate group could not be located due to disorder but the guanine was clearly seen, it appears that after cleavage of the phosphodiester bond, the resulting guanosine-3′-phosphate is not stabilized structurally in the active site. It is expelled, probably by rotation of the ribose from *syn* (substrate) to *anti* (product), and then guanine is removed from the recognition site and the product is released. In this interpretation, the RNase T_1–3′,5′-pGp complex represents the enzyme–product complex before dissociation into free enzyme and final product. Possible water-mediated hydrogen-bonding contacts between the 5′- and 3′-phosphate groups and protein atoms, both within the complex and with symmetry-related molecules, apparently provide sufficient stabilization to permit the unambiguous localization of the entire *anti*-3′,5′-pGp molecule. The required weakening of the substrate–enzyme interaction is also indicated by the insertion of two water molecules between the

Glu46 carboxylate and guanine N1, N2, and by the long and consequently weak guanine N2H···O Asn98 hydrogen bond of 3·3 Å (Table 4).

This work was supported by the Deutsche Forschungsgemeinschaft (Schwerpunkt 'Biophysik der Zelle') and Fonds der Chemischen Industrie. The authors are grateful to Luitpold-Werke, München, for generously providing the extract of *A. oryzae* used in this work.

References

ALTONA, C. & SUNDARALINGAM, M. (1972). *J. Am. Chem. Soc.* **94**, 8205–8212.
ARNI, R., HEINEMANN, U., TOKUOKA, R. & SAENGER, W. (1988). *J. Biol. Chem.* **263**, 15358–15368.
Biosym Technologies (1988). *DISCOVER User Manual.* Version 2.5. Biosym Technologies, San Diego, CA, USA.
Chemical Design Ltd (1990). *CHEMX.* Chemical Design Ltd, Oxford, England.
DATTAGUPTA, J. K., FUJIWARA, T., GRISHIN, E. V., LINDNER, K., MANOR, P. C., PIENIAZEK, N. J., SAENGER, W. & SUCK, D. (1975). *J. Mol. Biol.* **97**, 267–271.
FINZEL, B. C. (1987). *J. Appl. Cryst.* **20**, 53–55.
FITZGERALD, P. M. G. (1988). *J. Appl. Cryst.* **21**, 273–278.
FÜLLING, R. & RÜTERJANS, H. (1978). *FEBS Lett.* **88**, 279–282.
HEINEMANN, U. (1982). PhD Thesis, Univ. of Göttingen, Germany.
HEINEMANN, U. & HAHN, U. (1989). *Protein–Nucleic Acid Interaction*, edited by W. SAENGER & U. HEINEMANN, pp. 111–141. London: Macmillan.
HEINEMANN, U. & SAENGER, W. (1982). *Nature (London)*, **299**, 27–31.
HENDRICKSON, W. A. (1985). *Methods Enzymol.* **115**, 252–270.
HENDRICKSON, W. A. & KONNERT, J. H. (1980). *Computing in Crystallography*, edited by R. DIAMOND, S. RAMASESHAN & K. VENKATESAN, pp. 13.01–13.23. Bangalore: Indian Academy of Sciences.
HIRSCHFELD, F. L. (1968). *Acta Cryst.* A**24**, 301–311.
HOFFMANN, E., SCHMIDT, J., SIMON, J. & RÜTERJANS, H. (1988). *Nucleosides Nucleotides*, **7**, 757–761.
INAGAKI, F., SHIMADA, I. & MIYAZAWA, T. (1985). *Biochemistry*, **24**, 1013–1020.
JONES, T. A. (1978). *J. Appl. Cryst.* **11**, 268–272.
KENNARD, O. & HUNTER, W. N. (1989). *Q. Rev. Biophys.* **22**, 327–379.
KOEPKE, J., MASLOWSKA, M., HEINEMANN, U. & SAENGER, W. (1989). *J. Mol. Biol.* **206**, 475–488.
KOSTREWA, D., CHOE, H.-W., HEINEMANN, U. & SAENGER, W. (1989). *Biochemistry*, **28**, 7592–7600.
LESK, A. M. & HARDMAN, K. D. (1982). *Science*, **216**, 539–540.
MALIN, R., ZIELENKIEWICZ, P. & SAENGER, W. (1991). *J. Biol. Chem.* In the press.
MARTINEZ-OYANEDEL, J., CHOE, H.-W., HEINEMANN, U. & SAENGER, W. (1991). Submitted.
NORTH, A. C. T., PHILLIPS, D. C. & MATHEWS, F. S. (1968). *Acta Cryst.* A**24**, 351–359.
OSHIMA, T. & IMAHORI, K. (1972). *J. Biochem. (Tokyo)*, **70**, 197–199.
PAVLOVSKY, A. G. & KARPEISKY, M. Y. (1989). *Structure and Chemistry of Ribonucleases*, edited by A. PAVLOVSKY & K. POLYAKOV, pp. 303–314. Moscow: Academy of Sciences of the USSR.
RABINOVICH, D. & SHAKKED, Z. (1984). *Acta Cryst.* A**40**, 195–200.
ROSSMANN, M. G. (1972). Editor. *The Molecular Replacement Method.* New York: Gordon and Breach.
SAENGER, W. (1984). *Principles of Nucleic Acid Structure.* New York: Springer.
SHIMADA, I. & INAGAKI, F. (1990). *Biochemistry*, **29**, 757–764.
SUGIO, S., OKA, K.-I., OHISHI, H., TOMITA, K.-I. & SAENGER, W. (1985). *FEBS Lett.* **183**, 115–118.
TAKAHASHI, K. & MOORE, S. (1982). *The Enzymes*, **15**, 435–468.

Acta Cryst. (1991). B**47**, 527–535

Solution of the Structure of *Aspergillus niger* Acid α-Amylase by Combined Molecular Replacement and Multiple Isomorphous Replacement Methods

BY R. L. BRADY, A. M. BRZOZOWSKI,* Z. S. DEREWENDA,† E. J. DODSON AND G. G. DODSON

Department of Chemistry, University of York, Heslington, York YO1 5DD, England

(*Received* 11 *September* 1990; *accepted* 6 *February* 1991)

Abstract

The crystal structure of *Aspergillus niger* acid α-amylase was solved by a combination of multiple isomorphous replacement and molecular replacement methods. The atomic coordinates of *Aspergillus oryzae* (TAKA) α-amylase (entry 2TAA in the Protein Data Bank) and experimental diffraction data from a new monoclinic crystal form of TAKA α-amylase, were used during the procedure. Sequence identity between the two proteins is approximately 80%. The atomic parameters derived from the molecular replacement solution were too inaccurate to initiate least-squares crystallographic refinement. The molecular model was extensively revised against the experimental electron density map calculated at 3 Å resolution. Subsequent crystallographic refinement of this model using synchrotron

* Permanent address: Department of Crystallography, Institute of Chemistry, University of Łódź, Łódź, Poland.

† Present address to which all correspondence should be sent: MRC Group in Protein Structure and Function, Department of Biochemistry, 474 Medical Sciences Building, University of Alberta, Edmonton, Canada T6G 2H7.

0108-7681/91/040527-09$03.00